Incommensurate stripe order in $La_{2-x}Sr_xNiO_4$ with $x=0.225$

J. M. Tranquada
Department of Physics, Brookhaven National Laboratory, Upton, New York 11973

D. J. Buttrey
Department of Chemical Engineering, University of Delaware, Newark, Delaware 19716

V. Sachan*
Materials Science Program, University of Delaware, Newark, Delaware 19716

(Received 19 January 1996; revised manuscript received 17 June 1996)

In recent studies of $La_{2-x}Sr_xNiO_4$ it has been suggested that ordering of the dopant-induced holes occurs only commensurately at special values of x, such as $\frac{1}{3}$ and $\frac{1}{2}$. Commensurate order of both charge and spin densities has also been found in a crystal with $x=0.20$. The present neutron scattering study of an $x=0.225$ crystal demonstrates that the spin and charge order can also be incommensurate. In fact, the incommensurability is temperature dependent, as observed previously in $La_2NiO_{4.125}$, indicating that such behavior is intrinsic to the doped NiO_2 layers and not dependent on ordering of the dopant ions. A careful analysis of the unusual variation of peak widths as a function of momentum transfer perpendicular to the planes shows that the charge- and spin-density modulations are tied to the lattice, with the shift in phase of the charge modulations from one layer to the next equal to exactly one in-plane lattice spacing. A comparison of results for a number of samples shows that the charge and spin ordering temperatures vary linearly with hole concentration, with charge order always occurring at higher temperature, clearly indicating that the ordering is driven by the charge. [S0163-1829(96)05742-6]

I. INTRODUCTION

The combined ordering of charge and spin is proving to be a common phenomenon in transition-metal oxides. In hole-doped La_2NiO_4, the first evidence for unusual magnetic correlations was obtained in a neutron diffraction study[1] on a single crystal of $La_{1.8}Sr_{0.2}NiO_{3.96}$; similar magnetic ordering was also observed[2] in $La_2NiO_{4.125}$. Indications of charge order in $La_{2-x}Sr_xNiO_4$ were found in electron diffraction[3] and transport measurements[4] on ceramic samples. Recent neutron diffraction studies[5,6] of a $La_2NiO_{4.125}$ crystal were the first to detect diffraction from both the magnetic and charge order in the same sample. Quantitative analysis of those measurements has firmly established that the order (at least below the magnetic ordering transition) consists of a stripe phase, in which hole-rich stripes act as antiphase domain boundaries between stripes of antiferromagnetically ordered Ni spins. Related work on $La_{2-x}Sr_xNiO_4$ crystals with $x=0.135$ and 0.20 has demonstrated that similar charge and spin stripe order occurs in the Sr-doped material.[7]

While some features of the order are now clear, many questions remain. For example, Cheong and co-workers[3,4] have suggested that ordering is restricted to special values of x, such as $\frac{1}{3}$ and $\frac{1}{2}$, where commensurability is possible. Further evidence that $x=\frac{1}{3}$ is special was provided in a recent thermodynamic study.[8] Our previous neutron scattering study[7] of a single crystal with $x=0.20$, although not at a special value of x, did show commensurate order, albeit with a short in-plane correlation length of ~ 40 Å. In contrast, the stripe order found in $La_2NiO_{4+\delta}$ is incommensurate, with the wave vector varying significantly with temperature.[5,6] The difference between the cases of Sr and O doping leads one to ask whether the incommensurability and temperature dependence of the ordering wave vector in the latter case might be associated with the three-dimensional (3D) order of the oxygen interstitials.

The present neutron scattering study of an $x=0.225$ crystal gives a definitive answer to this question. The stripe order is found to be clearly incommensurate, and the ordering wave vector shows a temperature dependence similar to the oxygen-doped sample. Thus, these features appear to be intrinsic to the doped NiO_2 planes, with the temperature dependence suggesting that competing interactions are involved in the ordering.

Given the incommensurability, one may ask about the phase of the charge modulation with respect to the lattice. A probe of the phase is given by the stacking order of the charge stripes. It has been shown previously[6] that the charge stripes align themselves from one layer to the next so as to minimize the long-range part of the Coulomb interaction. With an incommensurate wave vector, keeping stripes in one layer equally far from their nearest neighbors in the next layer requires that the phase of the charge modulation be arbitrary. Is this the case for the $x=0.225$ crystal? The answer turns out to be hidden in the unusual variation of peak widths measured as a function of momentum transfer perpendicular to the planes. A careful analysis of both the magnetic and charge-order scattering shows that the charge stripes do not have an arbitrary phase: They are tied to the lattice and can only shift by increments of the lattice spacing. This result is evidence that local interactions compete with long-range forces.

A final question concerns the driving force for the stripe

order. Cheong and co-workers[3,4] have emphasized the primary role of the charge, and the thermodynamic study by Ramirez *et al.*[8] supports this idea. We had originally thought the spin and charge order to occur simultaneously,[5] but, although the strength of dynamical magnetic correlations grows with the charge order, it is now clear that magnetic *order* occurs at a lower temperature. The dominant role of the charge becomes manifest when one looks at the doping dependence of the transition temperatures. Comparing results on various samples, we show that both the magnetic and charge-order transition temperatures vary linearly with hole concentration.

The rest of the paper is organized as follows. The next section contains a brief review of nomenclature and notation, followed by a description of experimental procedures. The results and analysis are presented in Sec. IV. Trends with hole concentration are discussed in Sec. V.

II. NOTATION

The average structure of the composition under study remains in the high-temperature tetragonal (HTT) phase (space group $I4/mmm$) down to at least 10 K; however, the charge and spin order are more easily described in a unit cell of size $\sqrt{2}a\times\sqrt{2}a\times c$ compared to the HTT cell. Hence, we chose to index diffraction features in terms of such a cell with corresponding space group $F4/mmm$.

Detailed descriptions of the spin and charge stripe-order model have been given elsewhere;[6,9] for the present purposes we note that the spin-density modulation is characterized by the wave vector

$$\mathbf{g}_\epsilon=(1+\epsilon,0,0), \tag{1}$$

where wave vector components are specified in reciprocal lattice units $(2\pi/a,2\pi/a,2\pi/c)$. If $\mathbf{G}$ is a reciprocal lattice point of the average structure, then superlattice peaks appear at $\mathbf{G}\pm\mathbf{g}_\epsilon$. Since Néel order in the planes is characterized by $\mathbf{Q}_{\rm AF}=(1,0,0)$, it follows that the magnetic peaks appear in pairs about $\mathbf{Q}_{\rm AF}$ split by $(\pm\epsilon,0,0)$. [Because of twinning of the modulated structure (it costs no extra energy to create a domain rotated by 90°) peaks also appear at $(0,\pm\epsilon,0)$ with respect to $\mathbf{Q}_{\rm AF}$.] In real space the corresponding spin structure consists of locally antiferromagnetic order with an overall sinusoidal modulation of period a/ϵ. The characteristic wave vector for the charge density modulation is

$$\mathbf{g}_{2\epsilon}=(2\epsilon,0,1), \tag{2}$$

corresponding to a real-space modulation period of $a/2\epsilon$, half that of the magnetic period.

III. EXPERIMENTAL PROCEDURES

The single-crystal sample was grown by radio frequency induction skull melting as described elsewhere.[11] The starting composition had a Sr concentration of $x=0.25$; however, electron microprobe analysis of the resulting large crystals showed that the actual Sr concentration was $x=0.225$. The conditions for controlling the oxygen stoichiometry were determined by thermogravimetric analysis as a function of annealing temperature and oxygen partial pressure.[12,13] Oxygen stoichiometry (i.e., $\delta=0.00$) in the present sample was

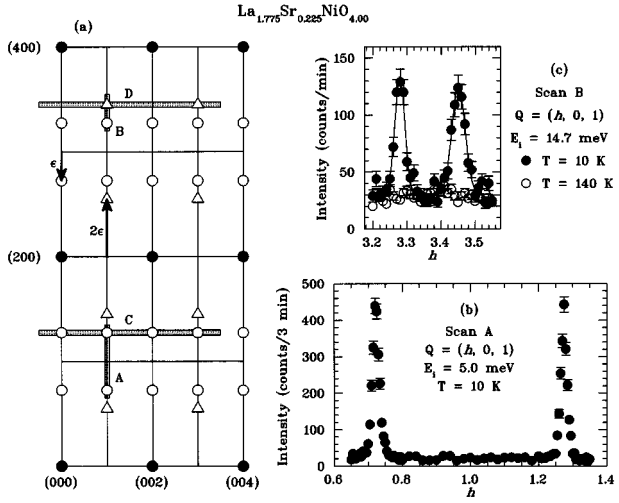

FIG. 1. (a) Diagram of the $(h0l)$ zone, showing positions of diffraction peaks, with indexing based on space group $F4/mmm$ for the average nuclear structure. Solid circles, fundamental Bragg peaks; open circles, magnetic superlattice peaks; open triangles, nuclear superlattice peaks corresponding to charge order. Shaded bars indicate ranges of representative scans of elastic scattering. (b) Scan A, through the magnetic peaks at $(1\pm\epsilon,0,1)$, at $T=10$ K. (c) Scan B, through the magnetic-order peak at $(3+\epsilon,0,1)$ and charge-order peak at $(4-2\epsilon,0,1)$, measured at $T=10$ K (solid circles) and 140 K (open circles).

achieved by a final annealing at $\sim$800 °C in 1 bar O_2. Preliminary neutron diffraction measurements indicated that the sample contained several crystals with different orientations. For the work reported below, a crystal block of volume $\sim$0.1 cm^3 was chipped from the bulk sample.

The neutron scattering measurements utilized the H9A and H7 triple-axis spectrometers at Brookhaven National Laboratory's High-Flux Beam Reactor. At H9A, which is on the cold source, neutrons of energy 5.0 meV were selected. Typical effective horizontal collimations of 40′-30′-80′-80′ (from reactor to detector) were used, along with a cold Be filter to eliminate neutrons at shorter harmonic wavelengths. At H7, a neutron energy of 14.7 meV, horizontal collimations of 40′-40′-40′-40′, and two pyrolytic graphite (PG) filters were used. At both spectrometers the neutrons were monochromatized and analyzed by PG crystals set for the (002) reflection. The 5 meV neutrons at H9 were exploited to study the magnetic scattering peaks, which are strongest at small momentum transfer Q, while the higher-energy neutrons at H7 where required to measure the nuclear scattering associated with charge order.

Most of the measurements were performed with the crystal oriented to have its [010] axis vertical, so that the $(h0l)$ zone of reciprocal space was in the horizontal scattering plane. A few checks were also made in the $(hk0)$ zone. The aligned crystal was mounted in an Al can with He exchange gas that was attached to the cold finger of a Displex closed-cycle He refrigerator. The temperature was monitored with Si diode and Pt resistance thermometers to an accuracy of better than ±1 K. The lattice parameters at 10 K were measured to be $a=5.42$ Å and $c=12.64$ Å.

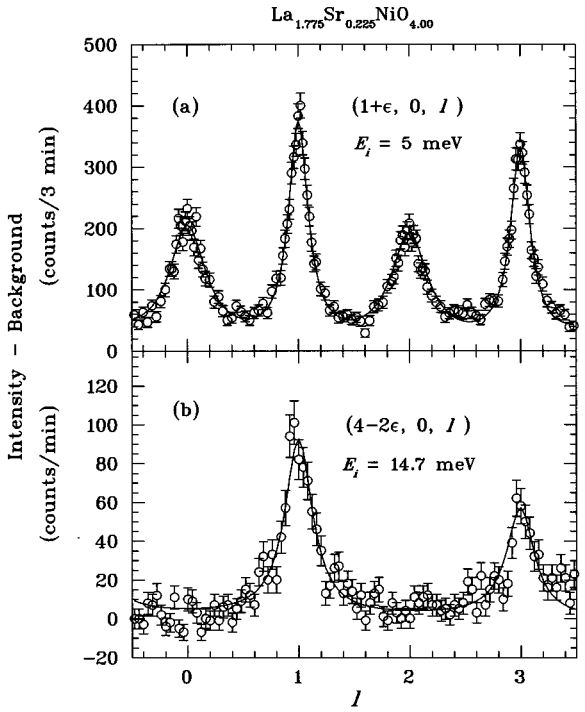

FIG. 2. (a) Scan C [see Fig. 1(a)] through magnetic peaks along $\mathbf{Q}=(1+\epsilon,0,l)$. (b) Scan D through charge-order peaks along $(4-2\epsilon,0,l)$. Both scans were measured at $T=10$ K, and the plotted intensity has been corrected for background. Solid lines are fits that are described in the text.

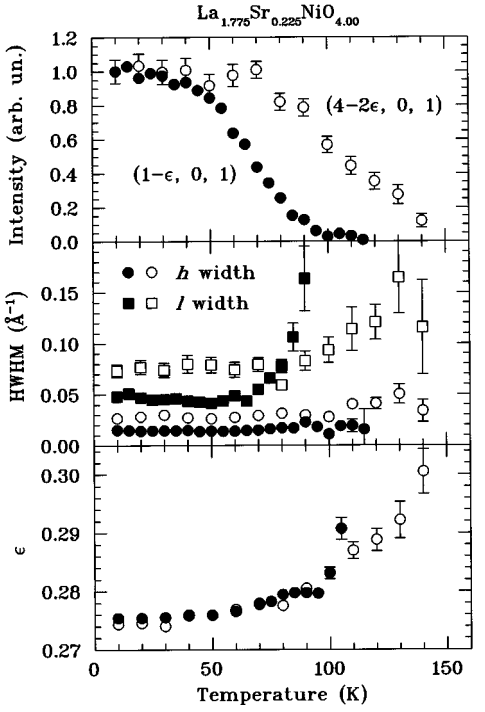

FIG. 3. Results for representative magnetic-order (solid symbols) and charge-order (open symbols) peaks as a function of temperature. Top panel: intensity integrated along h, where $\mathbf{Q}=(h,k,l)$. Middle panel: peak widths (half-width at half maximum) measured along h and l. The h widths are limited by resolution at low temperature. Bottom panel: incommensurate splitting parameter ϵ.

IV. EXPERIMENTAL RESULTS

A. Description

Figure 1(a) shows the positions within the $(h0l)$ zone of magnetic (open circles) and charge (open triangles) superlattice peaks associated with the three-dimensional stripe order observed[5,6,10] in $La_2NiO_{4+\delta}$ with $\delta=\frac{2}{15}$. In our previous study[7] of a $La_{2-x}Sr_xNiO_4$ crystal with $x=0.20$ we observed well-defined peaks of finite width when scanning along h through the superlattice points, but very broad diffuse scattering in scans along l. On increasing x to 0.225 we find that the peaks have sharpened considerably in both directions. Typical low-temperature h scans through magnetic and charge peaks [indicated as A and B in Fig. 1(a)] are shown in Figs. 1(b) and 1(c). A measurement of the $(1-\epsilon,0,1)$ magnetic peak with tighter horizontal collimations and lower-energy neutrons yielded a Lorentzian line shape with a half-width of 0.007 $Å^{-1}$. This corresponds to a correlation length of $\sim$150 Å. From the peak positions we find that, at low temperature, $\epsilon\approx0.275$, compared to 0.25 in the $x=0.20$ ($\delta=0.00$) crystal.

Scans along l through the magnetic and charge peaks [indicated as C and D in Fig. 1(a)] are shown in Fig. 2. Although the peaks are broad, they are very well resolved. (Note that the plotted intensity has been corrected for the background signal, so that the finite intensity between peaks is intrinsic.) As expected, magnetic peaks appear at all integer values of l, but charge-order peaks occur only when l is an odd integer; however, the variation of peak widths with l is quite unusual. For the magnetic scattering, the peaks at odd l are considerably sharper than those at even l, even though the integrated intensities of all peaks are essentially the same. The widths of the charge-order peaks are approximately equal to the average of the two magnetic widths. The analysis of the l-dependent scattering will be discussed below.

The temperature dependences of various peak parameters are presented in Fig. 3. The top panel shows the intensity integrated along h and normalized to 1 at 10 K; similar results are obtained by integrating l scans. One can see that the magnetic order disappears near 100 K, while the charge order does not approach zero until $\sim$150 K. The center panel shows the peak half-widths obtained from a Gaussian fit along h and a Lorentzian fit along l. (As will be shown below, the correct peak shape along l differs from a Lorentzian; nevertheless, the Lorentzian analysis is simple and gives an adequate description of the trend with temperature.) The h widths shown for both the magnetic and charge peaks are resolution limited below 100 K. The l widths clearly increase as the intensity decreases, suggesting a somewhat glassy transition, consistent with the lack of long-range order. The bottom panel presents the temperature dependence of the peak-position parameter ϵ, which increases as order is lost, in a manner similar to that found[5,6,10] in $La_2NiO_{4+\delta}$ with $\delta=\frac{2}{15}$.

To make the comparison with the oxygen-doped system more complete, we also checked the relative intensities of the $(1\pm\epsilon,0,0)$ and $(1,\pm\epsilon,0)$ magnetic peaks. For the $\delta=\frac{2}{15}$

phase the ratio of $|F|^2$ (where F is the structure factor) for the latter peaks to the former is approximately 0.065, which is consistent with having the spins lie in the plane pointed perpendicular to the modulation direction.[6] In contrast, the ratio for the $x=0.225$ crystal is 0.65. This larger ratio might indicate that, in the Sr-doped sample, there is a finite component of the spins parallel to the modulation direction, but it may also in some way be associated with the finite correlation length.

We have already commented on the temperature dependence of ϵ. One feature observed with the oxygen-doped samples, but not here, is a tendency for ϵ to lock in to certain rational fractions.[5,10] The particular fractions observed can be understood if the positions of ordered hole stripes within an NiO_2 plane are restricted by the lattice, with some of the stripes centered on Ni sites and the rest centered on oxygens.[10] Further evidence for pinning of the stripes by the lattice comes from the l dependence of the structure factors for the spin and charge superlattice peaks. Because of Coulomb repulsion, hole stripes in neighboring planes run parallel to each other with a staggered alignment, so as to maximize the spacing between nearest neighbors; however, pinning of the stripes to the lattice prevents an ideal staggering of stripe positions. An approximate staggering is achieved by shifting the stripe positions within one plane by one lattice spacing with respect to the nearest-neighbor planes. The l dependence of the structure factors is then given by

$$|F_n|^2 \sim 1+\cos(2\pi n\epsilon)\cos(\pi l), \tag{3}$$

where $n=1$ for the first-harmonic magnetic peaks and $n=2$ for the second-harmonic charge-order peaks. A related signature is present in the $x=0.225$ data, but some analysis is required to extract it. We present this analysis next.

B. Analysis

To analyze the l dependence of the spin- and charge-order scattering, we consider the problem of scattering from well-ordered layers with exponential decay of the correlations between layers. If F_n is the structure factor for the nth layer, then the scattered intensity is given by[14]

$$I=\sum_m (N-|m|)\langle F_n F^*_{n+m}\rangle e^{i\pi lm}, \tag{4}$$

where the layer spacing is taken to be $c/2$. If $\mathbf{Q}$ is of the form $(h,0,l)$, then for our problem it is possible to write

$$\langle F_n F^*_{n+m}\rangle = |F|^2 P_m. \tag{5}$$

For exponential decay of the correlations,

$$P_m = p^m, \tag{6}$$

with

$$|p| = e^{-c/2\xi}, \tag{7}$$

where ξ is the correlation length. Now, if we make the usual large-N approximation and ignore $|m|$ compared to N, then Eq. (4) becomes

$$I \approx N|F|^2 \sum_m p^m e^{i\pi lm} = N|F|^2 \frac{1-p^2}{1+p^2-2p\cos\pi l}. \tag{8}$$

This formula gives peaks at even integer l if p is positive, and peaks at odd integer l if p is negative. The width of the peak depends on p, while the integrated intensity (for a peak at $l=l_0$, integrated from $l_0-\frac{1}{2}$ to $l_0+\frac{1}{2}$) is independent of it.[14]

To make connection with experiment, first consider the case of $\epsilon=\frac{1}{4}$, which allows ideal staggering of the charge stripes and perfect stacking order. One then has, for the magnetic scattering,

$$P^s_m = \begin{cases} 1 & \text{for } m \text{ even,} \\ 0 & \text{for } m \text{ odd} \end{cases}$$
$$= \tfrac{1}{2}[(p_s)^m + (-p_s)^m], \tag{9}$$

with $p_s=1$, and, for the nuclear scattering associated with charge order,

$$P^c_m = \begin{cases} 1 & \text{for } m \text{ even,} \\ -1 & \text{for } m \text{ odd} \end{cases}$$
$$= (-p_c)^m, \tag{10}$$

again with $p_c=1$. These correlation factors give the proper extinction rules, i.e., magnetic peaks at both even- and odd-integer l but charge peaks only at odd-integer l.

If the stacking of stripe layers is the same as in the oxygen-doped samples, then for $\epsilon \neq \frac{1}{4}$ slightly more complicated expressions are required. For perfect correlations one has

$$P^s_m = \tfrac{1}{2}\{[1+\cos(2\pi\epsilon)](1)^m + [1-\cos(2\pi\epsilon)](-1)^m\} \tag{11}$$

and

$$P^c_m = \tfrac{1}{2}\{[1+\cos(4\pi\epsilon)](1)^m + [1-\cos(4\pi\epsilon)](-1)^m\}. \tag{12}$$

To introduce a finite correlation length, it would seem reasonable to replace the factors $(\pm 1)^m$ by $(\pm p)^m$; however, for the magnetic scattering this would cause the odd-integer and even-integer peaks to have different integrated intensities, which is inconsistent with experiment. We can satisfy the experimental constraint of uniform integrated intensities if, instead, we set

$$P^s_m = (p_{s+})^m + (-p_{s-})^m, \tag{13}$$

with

$$p_{s\pm} = p[1 \pm \cos(2\pi\epsilon)]. \tag{14}$$

This form corresponds to an increasing probability of stacking faults as a function of layer separation, m. For the charge peaks, we note that for the experimentally observed $\epsilon=0.275$ we have $\cos(4\pi\epsilon)=-0.95$, so that it should be sufficient to make use of Eq. (10). Assuming that the spin order and charge order have the same correlation length, this model then predicts that

$$p_{s+}/p_{s-} = 0.73 \tag{15}$$

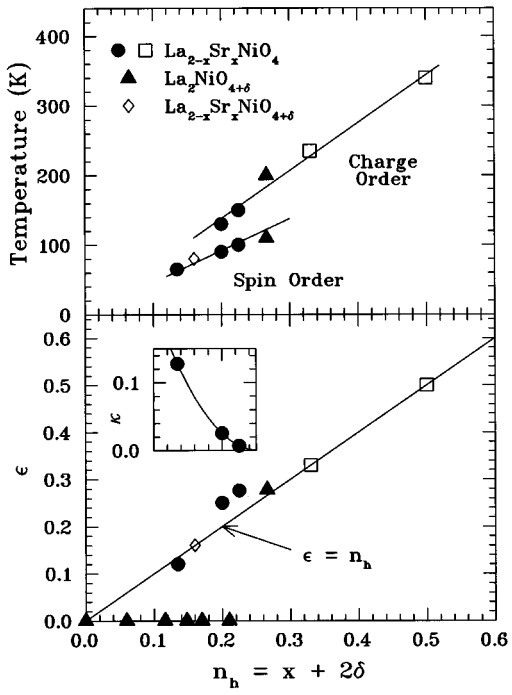

FIG. 4. Summary of results on charge and spin order for a number of doped La_2NiO_4 samples reported in the literature. Upper panel shows transition temperatures for charge and spin order, while lower panel shows incommensurability ϵ, all as a function of hole concentration n_h. Inset shows variation of the low-temperature inverse correlation length determined by neutron scattering for three $La_{2-x}Sr_xNiO_4$ crystals. Solid circles, present work and Ref. 7; solid triangles, Refs. 6 and 10; open squares, Ref. 3; open diamonds, Ref. 1.

and

$$(p_{s+}+p_{s-})/p_c=2. \tag{16}$$

We have fit the data using Eq. (8), in each case approximating $|F|^2$ by a slowly varying Gaussian and replacing N by a scale factor. The Gaussian width, scale factor, and p factors were varied to obtain the least-squares fits indicated by the lines in Fig. 2. The fits gave the parameter values $p_{s+}=0.531\pm0.007$, $p_{s-}=0.717\pm0.004$, and $p_c=0.625\pm0.016$, yielding

$$p_{s+}/p_{s-}=0.74\pm0.01 \tag{17}$$

and

$$(p_{s+}+p_{s-})/p_c=2.00\pm0.05, \tag{18}$$

in excellent agreement with the model. From the value of p_c we obtain a correlation length $\xi=1.06c$, or approximately two layer spacings.

V. DISCUSSION

We have seen that, for the $x=0.225$ crystal, the charge orders first, with magnetic order following at a lower temperature. The primary role of the charge in driving the ordering becomes even clearer when one compares results from several different studies. In the upper panel of Fig. 4 we have plotted the charge and spin ordering temperatures that have been reported in various diffraction studies[1,3,4,7,6,10] of both Sr- and O-doped La_2NiO_4 as a function of the net dopant-induced hole concentration $n_h=x+2\delta$. (Note that determination of the net hole concentration requires accurate knowledge of both the Sr and O concentrations. The value of n_h for the $x=0.2$ sample studied by Hayden *et al.*[1] has been adjusted to account for oxygen deficiency, as discussed in Ref. 7.) Remarkably, we find that not only does the charge ordering temperature increase with n_h, it appears to do so linearly. The spin ordering temperature also appears to vary linearly with n_h, although with a smaller slope. It has been shown previously[6,15–17] that in $La_2NiO_{4+\delta}$ with $\delta<0.11$, where the magnetic order remains commensurate, the Néel temperature drops from 335 K at $\delta=0$ to 50 K at $\delta=0.105$. The increasing spin ordering temperatures in the stripe-ordered regime must be driven by the charge order.

The lower panel of Fig. 4 shows how the splitting parameter ϵ, measured at low temperature, varies with n_h. As we have noted previously,[7,9] the trend in the stripe-ordered regime is $\epsilon\approx n_h$, which is consistent with the calculations of Zaanen and Littlewood.[18] The deviations from this trend we believe to be real, and, along with the temperature dependence of ϵ, they suggest the importance of the long-range part of the Coulomb interaction. The inset in the figure shows the variation of the in-plane inverse correlation length κ as a function of n_h for the Sr-doped crystals that we have studied.[7] The line through the points is a quadratic fit; extrapolation suggests that $\kappa\rightarrow0$ near $n_h=0.25$. Surprisingly, this value of n_h corresponds fairly closely to the point at which the magnetic order in the oxygen-doped nickelate changes from commensurate to stripes. The latter behavior is also correlated with a change in the dimensionality of the interstitial order from 1D to 3D. Perhaps these correspondences are more than a mere coincidence.

The analysis of Zaanen and Littlewood[18] suggests that one should think of holes that bind to domain walls within an antiferromagnetic background. This picture strongly influenced our previous discussions of stripe order;[5–7] however, the fact that the charge orders first is more consistent with the charge segregation concept of Emery and Kivelson.[19,20] The observation[7] that the low-energy magnetic spectral weight falls off as the charge order disappears indicates that without charge order the antiferromagnetic correlations disappear. Local antiferromagnetic order can occur only after the charge has segregated into hole-rich and hole-poor regions. The long-range part of the Coulomb interaction should suppress true phase separation and influence the stripe order.[20,21]

Competition between Coulomb and magnetic interactions can qualitatively explain the temperature dependence of the splitting parameter ϵ shown in Fig. 3. The local electronic and magnetic interactions presumably favor $\epsilon=n_h$, as suggested by the Hubbard model analysis.[18] On the other hand,

the Madelung energy is proportional to $|\mathbf{g}_{2\epsilon}|^{-2}$, and hence it is reduced by increasing ϵ. As the magnetic order disappears, the Madelung energy should become relatively more important, leading to an increase in ϵ as observed.

The trends indicated in Fig. 4 suggest that the charge ordering phenomenon is not necessarily restricted to special hole concentrations; however, it is possible that the ordering transition becomes sharper when the stripe modulation has a short-period commensurability. The rounded transitions in our $x=0.225$ sample are presumably due to the frustrating effects of the random potential associated with the Sr ions. A short-period commensurability might also enhance the effective coupling of the charge modulation to the lattice. Further diffraction investigations of stripe order (especially the magnetic component) in the $x \geqslant 0.25$ regime are needed.

ACKNOWLEDGMENTS

Helpful discussions with V. J. Emery and P. Wochner are gratefully acknowledged. Work at Brookhaven was carried out under Contract No. DE-AC02-76CH00016, Division of Materials Sciences, U.S. Department of Energy.

*Present address: Rodel, Inc., 451 Bellevue Road, Newark, Delaware 19713.

[1] S. M. Hayden *et al.*, Phys. Rev. Lett. **68**, 1061 (1992).
[2] K. Yamada *et al.*, Physica C **221**, 355 (1994).
[3] C. H. Chen, S.-W. Cheong, and A. S. Cooper, Phys. Rev. Lett. **71**, 2461 (1993).
[4] S.-W. Cheong *et al.*, Phys. Rev. B **49**, 7088 (1994).
[5] J. M. Tranquada, D. J. Buttrey, V. Sachan, and J. E. Lorenzo, Phys. Rev. Lett. **73**, 1003 (1994).
[6] J. M. Tranquada, J. E. Lorenzo, D. J. Buttrey, and V. Sachan, Phys. Rev. B **52**, 3581 (1995).
[7] V. Sachan *et al.*, Phys. Rev. B **51**, 12742 (1995).
[8] A. P. Ramirez *et al.*, Phys. Rev. Lett. **76**, 447 (1996).
[9] J. M. Tranquada, Ferroelectrics **177**, 43 (1996).
[10] P. Wochner, J. M. Tranquada, D. J. Buttrey, and V. Sachan (unpublished).
[11] D. J. Buttrey, H. R. Harrison, J. M. Honig, and R. R. Schartman, J. Solid State Chem. **54**, 407 (1984).
[12] D. J. Buttrey, V. Sachan, J. M. Tranquada, and J. E. Lorenzo, in *Advances in Superconductivity VII (ISTEC)*, edited by Yamafuji and Morishita (Springer-Verlag, Tokyo, 1995), pp. 351–356.
[13] V. Sachan, Ph.D. thesis, University of Delaware, (1995).
[14] A. Guinier, *X-Ray Diffraction in Crystals, Imperfect Crystals, and Amorphous Bodies* (Dover, New York, 1994).
[15] J. Rodríguez-Carvajal, M. T. Fernández-Díaz, and J. L. Martínez, J. Phys. Condens. Matter **3**, 3215 (1991).
[16] S. Hosoya *et al.*, Physica C **202**, 188 (1992).
[17] P. Gopalan *et al.*, Phys. Rev. B **45**, 249 (1992).
[18] J. Zaanen and P. B. Littlewood, Phys. Rev. B **50**, 7222 (1994).
[19] V. J. Emery and S. A. Kivelson, Physica C **209**, 597 (1993).
[20] S. A. Kivelson and V. J. Emery, in *Strongly Correlated Electronic Materials: The Los Alamos Symposium 1993*, edited by K. S. Bedell *et al.* (Addison-Wesley, Reading, MA, 1994), pp. 619–656.
[21] U. Löw, V. J. Emery, K. Fabricius, and S. A. Kivelson, Phys. Rev. Lett. **72**, 1918 (1994).